Data-driven Control of Distributed Energy Resources in Virtual Power Plants Under Uncertainty

Fatemeh Shojaei
School of Engineering
RMIT University
Melbourne, Australia
s3970924@student.rmit.edu.au

Arash Vahidnia
School of Engineering
RMIT University
Melbourne, Australia
arash.vahidnia@rmit.edu.au

Ali Moradi Amani
School of Engineering
RMIT University
Melbourne, Australia
ali.moradiamani@rmit.edu.au

***Abstract*—This study presents a data-driven control methodology for managing distributed energy resources (DERs)—specifically battery energy storage systems (BESS) and photovoltaic (PV) units—to improve the operational performance and reliability of virtual power plants (VPPs). Instead of relying on an explicit mathematical model, the proposed controller utilizes historical input–output measurements to coordinate the actions of BESS, PV units, and electric vehicles (EVs) under uncertain and variable operating conditions. To handle uncertainty and operational constraints, a predictive optimization layer is incorporated, enabling the controller to adjust in real time to fluctuations in grid conditions. By using actual household demand, PV generation, and EV charging data, the approach accurately reflects system behavior without the need for detailed parameter estimation or model identification. Extensive simulations on a European low-voltage distribution test feeder demonstrate that the controller can efficiently schedule PV and BESS resources while achieving substantial improvements in voltage regulation. The results verify the method's robustness, scalability, and suitability for practical real-time deployment in modern distribution networks with high renewable and EV integration.**

***Index Terms*—Data-driven control, distributed energy resources (DER), battery energy storage systems (BESS), virtual power plants (VPP), uncertainty, electric vehicle (EV)**

I. Introduction

The rapid growth of renewable energy technologies—particularly PV generation and BESS—has introduced new operational challenges for modern distribution networks, with voltage regulation emerging as one of the most critical issues. While these resources contribute to system flexibility and lower environmental impact, their intermittent and uncertain behavior can disrupt the stability of unbalanced low-voltage grids [1]–[3]. As a result, advanced and intelligent control strategies have received increasing attention for enabling reliable and coordinated operation of DERs [4].

Traditional decentralized and offline control methods, although straightforward to implement, lack the responsiveness needed to address fast variations caused by renewable intermittency and EV charging demand. These limitations often lead to voltage deviations and operational inefficiencies in networks with high renewable penetration. In comparison, real-time BESS control offers the ability to regulate active power through rapid charging and discharging actions, which significantly enhances voltage stability and overall system reliability [3]–[5]. A variety of optimization-based frameworks have been proposed for DER coordination—including power-sharing mechanisms [6], real-time storage redispatch [7], and adaptive energy management approaches for hybrid EV systems [8], [9]. However, the majority of these methods depend on deterministic models or offline computations, limiting their effectiveness when facing uncertainty in PV and EV behavior [6]– [10].

Recent research trends emphasize adaptive and predictive strategies to better manage uncertainties. Notable examples include predictive control schemes for hybrid EVs [11], nonlinear MPC formulations for hybrid storage systems [12], and real-time control methods incorporating battery health monitoring [13]. Despite their advantages, these approaches still rely on accurate system models, which are difficult to obtain for highly nonlinear, uncertain, or time-varying distribution networks. This challenge has led to growing interest in data-driven and model-free control frameworks [14]. Although MPC remains a widely adopted tool for constrained control [15], its dependence on model accuracy can degrade performance under mismatch [16]. Similarly, reinforcement learning [17], online identification methods [18], [19], and other data-driven techniques [20] attempt to reduce modeling requirements but often struggle with data efficiency, safety guarantees, and constraint enforcement. Non-parametric predictive control approaches [21]– [24] mitigate some of these limitations, yet they frequently face challenges in managing operational constraints in practical environments.

To address these difficulties, this work employs Data-enabled Predictive Control (DeePC) [25], a model-free control paradigm that constructs predictive behaviors directly from previously measured input–output data. Within the VPP architecture, the proposed controller performs real-time coordination of PV units and BESS over a 5-minute sampling interval,

979-8-3315-8138-1

aiming to minimize net-load deviations, reduce control effort, and adhere to PV generation references while enforcing operational limits. These include BESS power and SOC constraints, PV availability bounds, and voltage magnitude limits derived from the network. Applied to a highly unbalanced European low-voltage test feeder with substantial renewable and EV penetration, the DeePC-based VPP controller demonstrates effective DER coordination, improved voltage regulation, and enhanced robustness under uncertainty.

The rest of this paper is structured as follows: Section I reviews relevant control strategies; Section II describes the mathematical formulation; Section III presents the case study and simulation results; and Section IV concludes the paper.

II. Mathematical Formulation

The DeePC framework offers a data-driven alternative to conventional feedback control by using measured input–output trajectories instead of explicit parametric models. Based on behavioral systems theory, it reconstructs system dynamics directly from historical data, eliminating the need for model identification or state estimation [25]. This makes DeePC particularly suitable for complex systems such as VPPs, where accurate modeling is difficult and uncertain. Unlike model-based MPC, DeePC computes control inputs directly from data, improving robustness to model mismatch and enhancing adaptability. For deterministic LTI systems, DeePC provides prediction performance comparable to classical MPC, ensuring similar closed-loop behavior [26]. In this work, the framework is implemented in discrete time with a 5-minute sampling interval, where the control input vector $u_k \in \mathbb{R}^m$ at time step k is defined as

$$u_k = \begin{bmatrix} u_k^{\text{PV}} \\ u_k^{\text{BESS}} \end{bmatrix}, \tag{1}$$

Here, $u_k^{\text{PV}} \in \mathbb{R}^{n_{\text{PV}}}$ and $u_k^{\text{BESS}} \in \mathbb{R}^{n_{\text{BESS}}}$ denote the active power commands for the PV units and BESS units. The output vector $y_k \in \mathbb{R}^p$ represents the measured net active power at the monitored buses and is given by

$$y_k = P_{\text{Household}} + P_{\text{EV}} - u_k^{\text{PV}} + u_k^{\text{BESS}}, \tag{2}$$

where positive values indicate grid import and negative values indicate export. $P_{\text{Household}}$ and P_{EV} correspond to household demand and EV charging load, respectively. Under the sign convention, $u_k^{\text{BESS}} > 0$ denotes charging and $u_k^{\text{BESS}} < 0$ denotes discharging. This expression links the controllable inputs u_k to the resulting net power injection y_k in the network.

A. Preliminaries on MPC

For reference, the dynamics of a standard discrete-time linear time-invariant (LTI) system can be written as

$$\begin{aligned} x_{k+1} &= Ax_k + Bu_k, \\ y_k &= Cx_k + Du_k, \end{aligned} \tag{3}$$

where $x_k \in \mathbb{R}^n$ represents the system state and (A, B, C, D) denote the corresponding system matrices. Model predictive control (MPC) determines the control sequence $\{u_k\}_{k=0}^{N-1}$ by minimizing a finite-horizon objective of the form

$$\begin{aligned} \min_{u_k, x_k, y_k} \; & \sum_{k=0}^{N-1} \left(\|y_k - y_k^{\text{ref}}\|_Q^2 + \|u_k\|_R^2 \right) \\ \text{s.t.} \; & x_{k+1} = Ax_k + Bu_k, \qquad y_k = Cx_k + Du_k, \\ & u_k \in \mathcal{U}, \;\; y_k \in \mathcal{Y}. \end{aligned} \tag{4}$$

While MPC ensures stability and constraint satisfaction when the system model is accurate, its performance can degrade significantly in the presence of model uncertainties or time-varying parameters [26]. This motivates the introduction of data-driven control approaches that do not rely on explicit system models.

B. Data-Enabled Predictive Control (DeePC)

DeePC removes the need for an explicit system model by relying entirely on measured input–output data. Let $u^d = \text{col}(u_1, \dots, u_T) \in \mathbb{R}^{Tm}$ and $y^d = \text{col}(y_1, \dots, y_T) \in \mathbb{R}^{Tp}$ denote previously collected input and output trajectories that are persistently exciting of a suitable order. From these data, the block Hankel matrix of depth L for the input sequence is constructed as

$$\mathcal{H}_L(u^d) = \begin{bmatrix} u_1 & \cdots & u_{T-L+1} \\ \vdots & \ddots & \vdots \\ u_L & \cdots & u_T \end{bmatrix}, \tag{5}$$

and a corresponding Hankel matrix $\mathcal{H}_L(y^d)$ is formed for the output data [25]. For a selected past horizon T_{ini} and prediction horizon N, the Hankel matrices are partitioned as

$$\begin{bmatrix} U_p \\ U_f \end{bmatrix} = \mathcal{H}_{T_{\text{ini}}+N}(u^d), \qquad \begin{bmatrix} Y_p \\ Y_f \end{bmatrix} = \mathcal{H}_{T_{\text{ini}}+N}(y^d), \tag{6}$$

where (U_p, Y_p) contain the past input–output information and (U_f, Y_f) encode the possible future behavior [25].

Given the most recent measurements $(u_{\text{ini}}, y_{\text{ini}})$, any admissible future trajectory over the prediction horizon can be written as a linear combination of the columns of these Hankel matrices. In practice, however, forecast errors—particularly those arising from variability in EV charging and PV generation—can introduce inconsistencies in the net-load data. To account for such uncertainties, slack variables are incorporated into the DeePC formulation, allowing the data-based constraints to tolerate prediction errors [2], [6]. Accordingly, the DeePC constraint becomes [31]

$$\begin{bmatrix} U_p \\ Y_p \\ U_f \\ Y_f \end{bmatrix} g_k = \begin{bmatrix} u_{\text{ini},k} \\ y_{\text{ini},k} \\ u_k \\ y_k \end{bmatrix} + \begin{bmatrix} \sigma_{u,k} \\ \sigma_{y,k} \\ 0 \\ 0 \end{bmatrix}, \tag{7}$$

where $\sigma_{u,k}$ and $\sigma_{y,k}$ compensate for errors or noise in the past input–output data. The vector g_k acts as a set of coefficients that parameterize all possible future input and output trajectories generated from the stored data.

979-8-3315-8138-1

C. Control Objective and Optimization Problem

The DeePC optimization problem seeks to determine the coefficient vector g that minimizes a structured quadratic cost while satisfying physical and network constraints:

$$
\begin{aligned}
\min_{g,\, s^+,\, s^-} \quad & \underbrace{\|y_k - y_k^{\text{ref}}\|_Q^2}_{\text{output tracking}} + \underbrace{\|u_k\|_R^2}_{\text{control effort}} + \underbrace{\lambda_g \|g_k\|_2^2}_{\text{regularization}} \\
& + \underbrace{\lambda_u \|\sigma_{u,k}\|_2^2 + \lambda_y \|\sigma_{y,k}\|_2^2}_{\text{data consistency}} \\
& + \underbrace{w_{\text{PV}} \|u_k^{\text{PV}} - \bar{u}_{\text{PV}}^{\text{base}}\|_2^2}_{\text{PV reference tracking}} + \underbrace{\rho_V \left(\|s^+\|_2^2 + \|s^-\|_2^2\right)}_{\text{voltage slack penalty}} \\
\text{s.t.} \quad & u_{\min} \le u_k^{\text{BESS}} \le u_{\max}, \qquad y_{\min} \le y_k \le y_{\max}, \\
& 0 \le u_k^{\text{PV}} \le \bar{u}_{\text{PV}}^{\text{cap}}, \\
& \text{SOC}_{\min} \le \text{SOC}_k \le \text{SOC}_{\max}, \\
& dV_{\min} \le R_v y_k + s^+ - s^- \le dV_{\max}, \qquad s^\pm \ge 0.
\end{aligned} \tag{8}
$$

D. Interpretation of the Objective Function

Each term in (8) serves a specific control or operational purpose:

- $|y_k - y^{\text{ref}}|_Q^2 = |Y_f g - y^{\text{ref}}|_Q^2$: tracks the desired output, minimizing deviations of net demand from the scheduled profile. $Q \succeq 0$ defines the relative weight of each output.
- $|u_k|_R^2 = |U_f g|_R^2$: limits excessive actuation of PV and BESS units for smoother control and longer equipment life. $R \succ 0$ is block diagonal, with higher weights on BESS components.
- $\lambda_g |g|_2^2$: regularizes g to reduce overfitting and improve numerical conditioning.
- $||\lambda_{y,k}||_2^2$ and $\lambda_u ||\sigma_{u,k}||_2^2$: ensure consistency between reconstructed and measured past trajectories, enhancing robustness to noise.
- $w_{\text{PV}} ||u_k^{\text{PV}} - \bar{u}_{\text{PV}}^{\text{base}}||_2^2$: limits unnecessary PV curtailment to maximize renewable utilization while respecting grid constraints. $\bar{u}_{\text{PV}}^{\text{base}}$ denotes the baseline PV forecast.
- $\rho_V(||s^+||_2^2 + ||s^-||_2^2)$: penalizes soft voltage constraint violations via slack variables, maintaining feasibility and power quality. This part is explained more in (11)-(13).

E. Physical and Network Constraints

The control inputs must satisfy operational limits. For PV units, the available active power is constrained by the instantaneous irradiance:

$$0 \le u_k^{\text{PV}} \le \bar{u}_{\text{PV},k}^{\text{cap}}, \tag{9}$$

where $\bar{u}_{\text{PV},k}^{\text{cap}}$ is obtained from the measured or forecasted PV output at each 5-minute interval.

For BESS units, both power and energy constraints are imposed as

$$
\begin{aligned}
& P_{\min} \le u_k^{\text{BESS}} \le P_{\max}, \\
& \text{SOC}_{k+1} = \text{SOC}_k + \Delta T\, u_k^{\text{BESS}}, \\
& \text{SOC}_{\min} \le \text{SOC}_k \le \text{SOC}_{\max}.
\end{aligned} \tag{10}
$$

Voltage quality is maintained through a linearized sensitivity model [30]:

$$dV = R_v y_k = R_v Y_f g, \tag{11}$$

where R_v is computed offline from the network impedance matrix. Voltage magnitudes are constrained by

$$dV_{\min} \le R_v Y_f g \le dV_{\max}, \tag{12}$$

with limits derived from the permissible range $(0.95, 1.05)$ p.u.

To accommodate model mismatch, slack variables s^+ and s^- are added:

$$dV_{\min} \le R_v Y_f g + s^+ - s^- \le dV_{\max}, \qquad s^\pm \ge 0, \tag{13}$$

and their penalties $\rho_V(\|s^+\|_2^2 + \|s^-\|_2^2)$ discourage unnecessary voltage violations.

III. Case Study and Results

This case study investigates an unbalanced European low-voltage distribution feeder operated as a VPP [27], [28] (Fig. 1). The aim is to implement a data-driven control strategy capable of coordinating PV generation and BESS charging/discharging across the network in real time.

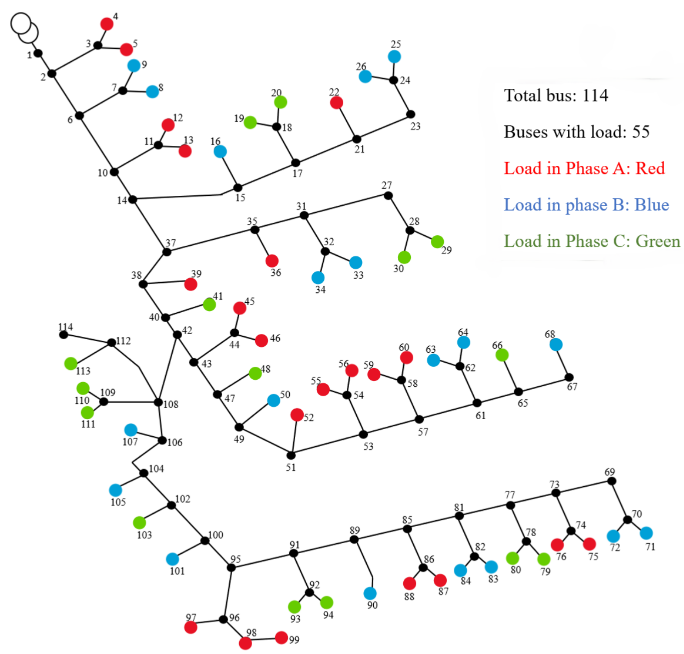

Fig. 1: IEEE European low-voltage distribution network.

PV systems are installed at every load bus, while 25% of the buses are randomly assigned BESS units and 50% host EVs, each following one of four representative charging profiles (Fig. 2) [29]. The PV traces in Fig. 2 represent the baseline forecasted generation for all PV units.

To incorporate uncertainty in EV charging behavior, a scenario-based stochastic approach is adopted. In line with [29], EV availability is modeled with a normally distributed random factor exhibiting a 42.5% variability. The

979-8-3315-8138-1

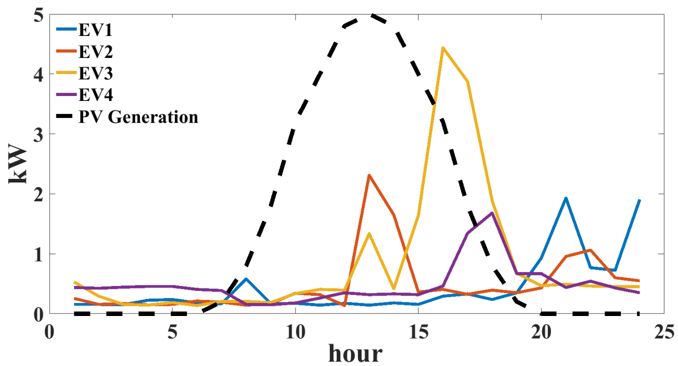

Fig. 2: EV and PV generation profiles.

controller simultaneously regulates PV output and BESS power to follow a predefined net-load reference, reduce PV curtailment, and satisfy all physical and network constraints using measured input–output data.

The control input vector u_k includes PV dispatch and BESS charge/discharge rates, bounded by

$$-5 \le u_k^{\text{BESS}} \le 5, \qquad 0 \le u_k^{\text{PV}} \le 5 \text{ kW}, \quad \forall k.$$

Each BESS has an energy capacity between 0 and 20 kWh. Its SOC follows (10) and is required to satisfy

$$0 \le SOC_k \le 20 \text{ kWh}, \quad \forall k.$$

Voltage magnitudes across all buses must remain within the standard 0.95–1.05 p.u. limits. To ensure feasible power adjustments throughout the simulation, all BESS units start with an SOC of 10 kWh. A 5-minute sampling interval is used for all control computations.

The dataset contains $T = 600$ samples, corresponding to 70 intervals of 12 samples each. The DeePC configuration uses a past horizon of $T_{\text{ini}} = 24$ samples and a prediction horizon of $N = 1$, giving $L = T - T_{\text{ini}} - N + 1$ Hankel columns. The full simulation lasts for $24 \times 12 = 312$ steps, representing a complete 24-hour period.

Weekend household net-load profiles under mild conditions are extracted from smart-meter data from 1,120 homes in Victoria, Australia (July 2018 – March 2020) [30]. Representative consumption levels and the reference trajectory used for controller design are provided in Table I.

TABLE I: Household consumption and output reference values

Time interval	Household consumption (kW)	Reference net load (kW)
12am–6am	0.2–0.3	0.15
6am–8am	0.2–0.4	0.1
8am–1pm	0.4–0.5	-0.4
1pm–4pm	0.4–0.5	-0.35
4pm–7pm	0.4–0.7	-0.165
7pm–12am	0.4–0.7	0.3

The controller's performance is assessed using 5-minute voltage variations. In the absence of control, PV injections cause voltages—especially between buses 40 and 68 on phase A—to surpass the 1.05 p.u. threshold during midday (Fig. 3(a)). Incorporating EV charging increases local demand, resulting in slightly lower voltage levels (Fig. 3(b)). When the proposed DeePC controller is applied, coordinated PV and BESS actions significantly reduce voltage deviations and maintain all magnitudes within acceptable limits (Fig. 3(c)). The green dashed regions highlight periods where overvoltage occurs.

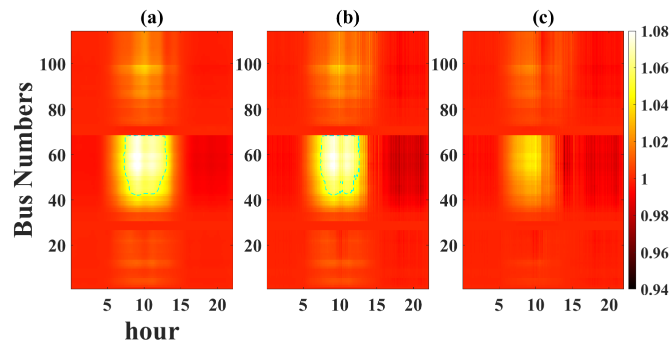

Fig. 3: Voltage heat maps of 114 buses (Phase A): (a) Household + PV (No Control), (b) Household + EV + PV (No Control), (c) Household + EV + PV + BESS (Controlled).

Figure 4(a-1) illustrates the mean PV generation (yellow) and BESS power (blue), while Fig. 4(a-2) compares the resulting net output against the reference. The average SOC evolution of all BESS units is shown in Fig. 4(b). Overall, the controller achieves coordinated DER operation, limits unnecessary PV curtailment, and maintains SOC trajectories within feasible bounds. The shaded regions denote the operating ranges of all PV units, BESS units, and SOC trajectories across the network.

IV. Conclusion

This paper presented a data-driven control framework for coordinated management of DERs in VPPs, focusing on the real-time operation of PV units, BESS, and EVs. By adopting the DeePC approach, the proposed controller eliminates the dependence on explicit system models and leverages historical input–output data to predict and optimize system behavior under uncertainty. The predictive optimization structure enables dynamic adaptation to grid fluctuations while enforcing operational constraints on voltage, power, and state of charge. Simulation results on an unbalanced European low-voltage distribution network verified the effectiveness of the proposed strategy. The DeePC-based VPP controller successfully coordinated BESS and PV operations, mitigated voltage deviations, and enhanced overall system reliability. The outcomes demonstrate that the proposed method is robust, scalable, and practically applicable for real-time deployment in modern data-rich power systems with high renewable and EV penetration.

References

[1] J. Lersch, R. Tang, M. Weibelzahl, J. Weissflog, and Z. Wu, "Assessing the impacts of energy sharing on low voltage distribution networks:

979-8-3315-8138-1

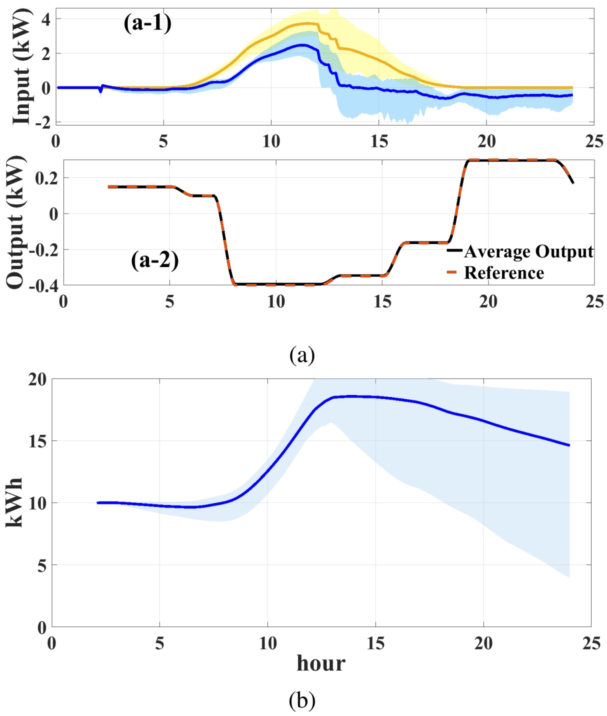

Fig. 4: (a-1) Average PV generation (yellow) and BESS power (blue). (a-2) Net output vs. reference. (b) Average SOC of BESS units.

Insights into electrification and electricity pricing in Germany," *Appl. Energy*, vol. 378, p. 124743, 2025.

[2] P. Srivastava, R. Haider, V. J. Nair, V. Venkataramanan, A. M. Annaswamy, and A. K. Srivastava, "Voltage regulation in distribution grids: A survey," *Annu. Rev. Control*, vol. 55, pp. 165–181, 2023.

[3] C. Guo, X. Wang, Y. Zheng, and F. Zhang, "Real-time optimal energy management of microgrid with uncertainties based on deep reinforcement learning," *Energy*, vol. 238, p. 121873, 2022.

[4] Z. Chen, A. M. Amani, X. Yu, and M. Jalili, "Control and optimisation of power grids using smart meter data: A review," *Sensors*, vol. 23, no. 4, p. 2118, 2023.

[5] W. Tang, Y. Huang, T. Qian, C. Wei, and J. Wu, "Coordinated central-local control strategy for voltage management in PV-integrated distribution networks considering energy storage degradation," *Appl. Energy*, vol. 389, p. 125684, 2025.

[6] B. Yildirim, M. A. Elgendy, A. Smith, and V. Pickert, "Efficiency optimized power sharing algorithm for modular battery energy storage systems," *IEEE Trans. Ind. Electron.*, 2022.

[7] P. A. Dratsas, G. N. Psarros, and S. A. Papathanassiou, "A real-time redispatch method to evaluate the contribution of storage to capacity adequacy," *IEEE Trans. Power Syst.*, 2023.

[8] G. Mathesh and R. Saravanakumar, "A novel intelligent controller-based power management system with instantaneous reference current in hybrid energy-fed electric vehicle," *IEEE Access*, 2023.

[9] X. Li and S. Wang, "Energy management and operational control methods for grid battery energy storage systems," *CSEE J. Power Energy Syst.*, vol. 7, no. 5, pp. 1026–1040, 2019.

[10] A. M. Ali, B. Moulik, and D. Söffker, "Intelligent real-time power management of multi-source HEVs based on driving state recognition and offline optimization," *IEEE Trans. Intell. Transp. Syst.*, vol. 24, no. 1, pp. 247–257, 2022.

[11] C. Jia, W. Qiao, J. Cui, and L. Qu, "Adaptive model-predictive-control-based real-time energy management of fuel cell hybrid electric vehicles," *IEEE Trans. Power Electron.*, vol. 38, no. 2, pp. 2681–2694, 2022.

[12] P. Golchoubian and N. L. Azad, "Real-time nonlinear model predictive control of a battery–supercapacitor hybrid energy storage system in electric vehicles," *IEEE Trans. Veh. Technol.*, vol. 66, no. 11, pp. 9678–9688, 2017.

[13] L. Timilsina *et al.*, "A real-time prognostic-based control framework for hybrid electric vehicles," *IEEE Access*, vol. 11, pp. 127589–127607, 2023.

[14] Z. S. Hou and Z. Wang, "From model-based control to data-driven control: Survey, classification and perspective," *Information Sciences*, vol. 235, pp. 3–35, 2013.

[15] J. B. Rawlings and D. Q. Mayne, *Model Predictive Control: Theory and Design*. Nob Hill Publishing, 2009.

[16] H. Hjalmarsson, "From experiment design to closed-loop control," *Automatica*, vol. 41, no. 3, pp. 393–438, 2005.

[17] B. Recht, "A tour of reinforcement learning: The view from continuous control," *arXiv preprint* arXiv:1806.09460, 2018.

[18] M. C. Campi and E. Weyer, "Finite sample properties of system identification methods," *IEEE Trans. Autom. Control*, vol. 47, no. 8, pp. 1329–1334, 2002.

[19] S. Dean, H. Mania, N. Matni, B. Recht, and S. Tu, "On the sample complexity of the linear quadratic regulator," *arXiv preprint* arXiv:1710.01688, 2017.

[20] F. Berkenkamp, M. Turchetta, A. Schoellig, and A. Krause, "Safe model-based reinforcement learning with stability guarantees," in *Advances in Neural Information Processing Systems*, 2017, pp. 908–918.

[21] R. W. Freedman and A. Bhatia, "Adaptive dynamic matrix control: Online evaluation of the DMC model coefficients," in *Proc. American Control Conf.*, IEEE, 1985, pp. 220–225.

[22] P. Lundstrom, J. H. Lee, M. Morari, and S. Skogestad, "Limitations of dynamic matrix control," *Comput. Chem. Eng.*, vol. 19, no. 4, pp. 409–421, 1995.

[23] I. Markovsky and P. Rapisarda, "Data-driven simulation and control," *Int. J. Control*, vol. 81, no. 12, pp. 1946–1959, 2008.

[24] W. Favoreel, B. De Moor, P. Van Overschee, and M. Gevers, "Model-free subspace-based LQG-design," in *Proc. American Control Conf.*, vol. 5, IEEE, 1999, pp. 3372–3376.

[25] J. Coulson, J. Lygeros, and F. Dörfler, "Data-enabled predictive control: In the shallows of the DeePC," in *Proc. 18th Eur. Control Conf. (ECC)*, Naples, Italy, Jun. 2019, pp. 307–312.

[26] E. F. Camacho and C. B. Alba, *Model Predictive Control*. Springer Science & Business Media, 2013.

[27] M. A. Khan and B. P. Hayes, "A reduced electrically equivalent model of the IEEE European low voltage test feeder," in *Proc. IEEE Power Energy Soc. Gen. Meeting (PESGM)*, 2022, pp. 1–5.

[28] P. Arboleya, A. Koirala, L. Suárez-Ramón, and B. Mohamed, "Non-synthetic European low voltage test system," 2018. [Online]. Available: https://ieeexplore.ieee.org/document/xxxxxxx

[29] A. Ostermann and T. Haug, "Probabilistic forecast of electric vehicle charging demand: Analysis of different aggregation levels and energy procurement," *Energy Informatics*, vol. 7, no. 1, p. 13, 2024.

[30] A. M. Amani, S. S. Sajjadi, N. Al Khafaf, H. Song, M. Jalili, X. Yu, and P. McTaggart, "Technology balancing for reliable EV uptake in distribution grids: An Australian case study," *Renew. Energy*, vol. 206, pp. 939–948, 2023.

[31] Y. Zhao, T. Liu, and D. J. Hill, "A data-enabled predictive control method for frequency regulation of power systems," in *Proc. IEEE PES Innovative Smart Grid Technologies Europe (ISGT Europe)*, Oct. 2021, pp. 1–6.